Eur. Phys. J. B **27**, 385–392 (2002)
DOI: 10.1140/epjb/e2002-00169-x

THE EUROPEAN PHYSICAL JOURNAL B

Investigation of excitation energies and Hund's rule in open shell quantum dots by diffusion Monte Carlo

L. Colletti[1], F. Pederiva[2,a], E. Lipparini[2], and C.J. Umrigar[3]

[1] Lawrence Livermore National Laboratory, Livermore, CA 94551-0808, USA
[2] Dipartimento di Fisica and INFM, Università di Trento, via Sommarive 14, 38050 Povo, Trento, Italy
[3] Cornell Theory Center, Cornell University, Ithaca, NY 14853, USA

Received 20 November 2001 and Received in final form 20 February 2002
Published online 6 June 2002 – © EDP Sciences, Società Italiana di Fisica, Springer-Verlag 2002

Abstract. We use diffusion Monte Carlo to study the ground state, the low-lying excitation spectrum and the spin densities of circular quantum dots with parabolic radial potentials containing $N = 16$ and $N = 24$ electrons, each having four open-shell electrons and compare the results to those obtained from Hartree-Fock (HF) and density functional local spin density approximation (LSDA) calculations. We find that Hund's first rule is obeyed in both cases and that neither HF nor LSDA correctly predict the ordering of the energy levels.

PACS. 73.21.La Electron states in quantum dots

1 Introduction

It is possible to make solid-state structures, called quantum dots, at semiconductor interfaces that confine a small number of mobile electrons. Quantum dots [1–4], containing one to several tens of electrons are analogous to atoms with tunable properties, exhibiting shell structure and obeying Hund's first rule. They are both of considerable technological interest and of theoretical interest because it is possible to go from a weak correlation to a strong correlation regime by tuning the relative strength of the external potential to the electron-electron potential.

A variety of theoretical methods have been used to study the electronic structure of quantum dots. Some of the simpler methods that have been used are the (spin-unrestricted) Hartree-Fock method (HF) and the space- and spin-unrestricted Hartree-Fock method (UHF) [5,6], that treat exchange exactly but totally ignore correlation, and the local spin density approximation (LSDA) and its space-unrestricted version, ULSDA [7,8], to density functional theory that treat both exchange and correlation approximately. In contrast to the situation in atoms, where the exchange energy is much larger than the correlation energy, in dots it is possible to be in a low density regime where exchange and correlation are equally important. Consequently it has been found [9,10] that in contrast to atoms, the Hartree-Fock approximation is a poor approximation for dots and that the local spin density approximation is significantly better but nevertheless inadequate for predicting the correct ordering and values of the ground and excited state energies. Another disadvantage of the local spin density approximation is that the wave functions are not eigenstates of total spin $\hat{S}^2$. The configuration interaction or exact diagonalization method [11–14] has the advantage of being systematically improbable but suffers from an exponential increase in the computer time as a function of the number of electrons for fixed accuracy in the energy. Hence this method in practice yields accurate energies for only $N \leq 6$ electrons. Some of the most accurate results to date have been obtained by the stochastic variational method with correlated Gaussian basis functions [15], but this method too scales badly with N and is limited to a similar or slightly larger number of electrons. Another method that has been used [16,17] is the path-integral Monte Carlo method but it has the disadvantage that one cannot differentiate between states that differ only in the orbital angular momentum, L, quantum number. Instead, the diffusion Monte Carlo method is our method of choice because it offers the best compromise between computational time and accuracy. For bosonic ground states it yields essentially exact results, aside from statistical errors. For fermionic states it suffers from the "fixed-node error" but this error can in many cases be made very small by choosing well optimized trial wave functions. In our earlier work [9], we calculated ground and low-lying excited states of dots with $N \leq 13$ electrons. The energies of ground and excited states with $N \leq 6$ electrons were checked by the stochastic variational method [15] and excellent agreement was found for all states except one [18].

[a] e-mail: pederiva@science.unitn.it

In Section 2 we describe the computational methods we use, in Section 3 we present ground and excited state energies and ground state spin densities of $N = 16$ and $N = 24$ dots. The conclusions are in Section 4.

2 Computational method

2.1 Hamiltonian

We model the dot as usual within the effective mass approximation as N electrons in a 2-dimensional space ($z = 0$ plane), whose motion is laterally confined by the potential $V_{\rm con}(\mathbf{r}) = \omega^2 r^2/2$. The Hamiltonian is

$$H = \sum_{i=1}^{N} \left(-\frac{\hbar^2}{2m^*}\nabla_i^2 + V_{\rm con}(\mathbf{r}_i) \right) + \frac{\mathrm{e}^2}{\epsilon} \sum_{i<j}^{N} \frac{1}{|\mathbf{r}_i - \mathbf{r}_j|}, \quad (1)$$

where m^* is the electron effective mass, and ϵ is the dielectric constant of the semiconductor. For GaAs $m^* = 0.067 m_e$, where m_e is the electron mass, and $\epsilon = 12.4$. Employing effective atomic units, ($\hbar = \frac{\mathrm{e}^2}{\epsilon} = m^* = 1$), the energies are in effective Hartree units and lengths in effective Bohr radii. For the GaAs parameters the effective Hartree is $\mathrm{H}^* = \mathrm{H} m^*/(m_e \epsilon^2) \simeq 11.86$ meV and the effective Bohr radius is $a_0^* = a_0 \epsilon m_e/m^* \simeq 97.93$ Å.

For parabolic quantum dots the single particle levels have energies [19] $\epsilon_{n,l} = (2n + |l| + 1)\omega$, where n is the principal quantum number and l is the azimuthal quantum number, and dots with electron numbers $N = 2, 6, 12, 20, 30, ...$ have closed-shell configurations. In both the dots we are considering, *i.e.*, $N = 16$ and $N = 24$, there are 4 electrons in a partially filled shell. The open-shell electrons occupy the $|n, l_z\rangle = |0, \pm 3\rangle, |1, \pm 1\rangle$ and the $|n, l_z\rangle = |0, \pm 4\rangle, |1, \pm 2\rangle, |2, 0\rangle$ orbitals in the $N = 16$ and $N = 24$ dots respectively.

The strength of the parabolic confinement depends on the number of electrons. A good approximation to the experimental dependency is given by $\omega^2 = \mathrm{e}^2/(\epsilon m^* r_s^3 \sqrt{N})$ where $r_s = 1/\sqrt{\pi \rho_0}$ is the Wigner–Seitz radius of a disk of uniform charge density ρ_0 whose potential approximates a parabola with spring constant ω at its center. For the $N = 16, 24$ dots we assume $r_s = 1.512$, and $r_s = 1.523$. The value of the confinement parameters are then $\omega = 0.269$ H* and 0.240 H* respectively, corresponding to energies of 3.2 and 2.9 meV.

2.2 Fixed-phase DMC

The diffusion Monte Carlo method employs the importance-sampled Green function

$$G(\mathbf{R}', \mathbf{R}, \tau) = \Psi_T(\mathbf{R}') \, \langle \mathbf{R}' | \mathrm{e}^{-\hat{H}\tau} \, | \mathbf{R} \rangle / \Psi_T(\mathbf{R}) \quad (2)$$

to project out the lowest state of the same symmetry as the trial state, $\Psi_T(\mathbf{R})$. As the projection time τ gets larger, the amplitude of higher states decay exponentially relative to the amplitude of the lowest state. Since $G(\mathbf{R}', \mathbf{R}, \tau)$ is not known exactly for general potentials, a short-time approximation is employed and the operator $\mathrm{e}^{-\hat{H}\tau}$ is applied repeatedly to achieve the desired projection and collect adequate statistics. In practice, we employ a slightly modified version of the propagator presented in reference [21] which has very small time-step errors.

In order to avoid a statistical error that grows exponentially with the projection time it is usual to employ the fixed-node [22] (for real wave functions) or the fixed-phase [23,24] (for complex wave functions) approximations to DMC, wherein one obtains the lowest state with the same nodes or the same phase as the trial state Ψ_T. For the lowest state of any symmetry, the energy obtained is an upper bound [25]. Our program is written to handle finite magnetic fields, in which case the wave function cannot be chosen to be real, so we employ the fixed-phase approximation.

It is always possible to split a complex-valued function Ψ_T into its modulus and phase:

$$\Psi_T(\mathbf{R}) = |\Psi_T(\mathbf{R})| \exp^{\mathrm{i}\phi_T(\mathbf{R})} , \quad (3)$$

where $\phi_T(\mathbf{R})$ is the phase function. The product

$$\Psi^*(\mathbf{R})\Psi_T(\mathbf{R}) = |\Psi(\mathbf{R})||\Psi_T(\mathbf{R})| \exp[\mathrm{i}(\phi_T(\mathbf{R}) - \phi(\mathbf{R}))] \quad (4)$$

cannot be used as the density for sampling, because it is not a positive definite function. In the fixed-phase approximation one assumes that

$$\exp[\mathrm{i}(\phi_T(\mathbf{R}) - \phi(\mathbf{R}))] = 1, \quad (5)$$

so the sampled distribution is

$$\rho = |\Psi(\mathbf{R})||\Psi_T(\mathbf{R})|. \quad (6)$$

2.3 Trial wave functions

Accurate DMC calculations in the fixed–node or fixed–phase approximations rely on the quality of the trial wave functions Ψ_T used for importance sampling. Our trial wave functions have the form

$$\Psi_T(\mathbf{R})_{L,S} = \exp[\phi(\mathbf{R})] \; \Xi^{L,S}(\mathbf{R}) , \quad (7)$$

where $\Xi^{L,S}(\mathbf{R})$ is the configuration-state function and $\exp[\phi(\mathbf{R})]$ is a generalized Jastrow factor.

The configuration state functions, Ξ_i, are eigenstates of the angular momentum $\hat{L}$, the total spin $\hat{S}^2$, and $\hat{S}_z$ of the form

$$\Xi^{L,S}(\mathbf{R}) = \sum_{j=1}^{m} \beta_j D_j^{\uparrow} D_j^{\downarrow} . \quad (8)$$

In equation (8), m is the number of determinants needed for the configuration state function, D_j are Slater determinants constructed from LSDA orbitals and β_j are the coefficients fixed by diagonalizing the S^2 operator in this determinantal basis. We prefer to employ LDA orbitals

Table 1. Comparison of the ground state energies (in effective Hartree units) of the the $N = 16$ and 24 dots obtained from DMC, VMC, LSDA and HF. The DMC and VMC ground states have quantum numbers $L=0, S=2$ following Hund's first rule. The numbers in parentheses are the statistical errors in the last digit.

		DMC/VMC	Energy (H^*)			
N	ω	L, S	DMC	VMC	LSDA	HF
16	0.269	0, 2	41.0460(4)	41.1217(8)	41.1091	42.2806
24	0.240	0, 2	75.9754(5)	76.117(1)	76.0102	77.9031

instead of LSDA orbitals, in order to facilitate the construction of eigenstates of $\hat{S}^2$. Details are provided in the Appendix. In one case (the ground state of the $N = 24$ dot) we used also wave functions [20] from a spatially unrestricted symmetry LSDA calculation (ULSDA), in which the density functional Hamiltonian is not restricted to have the circular symmetry that the true Hamiltonian possesses. In this case the orbitals do not transform as one of the irreducible representations of the 2-dimensional rotation group and the wave functions are not necessarily eigenstates of $\hat{L}$.

The generalized Jastrow factor has the form introduced in reference [26],

$$\phi(R) = \sum_{i=1}^{N} \sum_{k=1}^{6} \gamma_k J_0 \left(\frac{k\pi r_i}{R_c} \right) + \sum_{i<j}^{N} \frac{1}{2} \left(\frac{a_{ij} r_{ij}}{1 + b(r_i) r_{ij}} + \frac{a_{ij} r_{ij}}{1 + b(r_j) r_{ij}} \right) , \tag{9}$$

where

$$b(r) = b_{ij}^0 + b_{ij}^1 \tan^{-1} \frac{(r - R_c)^2}{2R_c \Delta} , \tag{10}$$

and $\gamma_k, b_{ij}^0, b_{ij}^1, \Delta$ and R_c are variational parameters. This function includes explicitly one- and two-body correlations, while the dependence of coefficients b on the position *via* equation (10) gives rise to implicit many body correlations. The a_{ij} coefficients are fixed by the cusp-condition, *i.e.*, the local energy defined as

$$E_L = \frac{\hat{H}\Psi_T}{\Psi_T}, \tag{11}$$

must remain finite when the distance r_{ij} between two electrons tends to zero. For a Coulomb system in two dimensions $a_{\uparrow\downarrow} = a_{\downarrow\uparrow} = 1$ and $a_{\uparrow\uparrow} = a_{\downarrow\downarrow} = 1/3$. The use of spin-dependent a_{ij} introduces spin contamination, *i.e.*, the wave functions are no longer strictly eigenstates of $\hat{S}^2$, but this contamination has been shown to be negligible in the case of atomic wave functions [27] and we expect that to be true here as well. All other coefficients in equation 10 are optimized by minimizing the variance of the local energy [28]. Typical values of the root mean square fluctuations of the local energy are $\sigma^2 = 0.3$–$0.4 H^*$, consistent with values found for smaller dots [9] if one assumes that to a rough approximation $\sigma \propto \sqrt{N}$. This suggests that the quality of the wavefunctions obtained is comparable to that of the smaller dots [9].

3 Results

3.1 Ground state results and Hund's first rules

In Table 1 we show ground state DMC and VMC energies. The DMC and VMC ground states of both dots have $L = 0, S = 2$ symmetry. The total spin S is the maximum allowed for four open-shell electrons, complying with Hund's first rule. For the $N = 24$ case, it is possible to form $|L=2, S=2\rangle$ and $|L=4, S=2\rangle$ states, but these have higher energies than the $|L=0, S=2\rangle$ state. Thus Hund's second rule, which states that the ground state angular momentum has the largest value consistent with Hund's first rule and fermion statistics, is not obeyed.

For the $N = 16$ dot, the occupied LSDA orbitals are $|n, l, s\rangle = |1, \pm 3, \frac{1}{2}\rangle$ and $|2, \pm 1, \frac{1}{2}\rangle$ resulting in a correct $|L = 0, S = 2\rangle$ prediction for the ground state symmetry. However, for the $N = 24$ dot the occupied LSDA orbitals are $|n, l, s\rangle = |1, \pm 4, \pm\frac{1}{2}\rangle$ resulting in an incorrect $|L = 0, S = 0\rangle$ prediction for the ground state symmetry. However, the $|L = 0, S = 2\rangle$ state with orbitals $|n, l, s\rangle = |1, \pm 4, \frac{1}{2}\rangle$ and $|1, \pm 2, \frac{1}{2}\rangle$ occupied is only $7 \times 10^{-6}\,\mathrm{H}^*$ higher in energy. These calculations were performed with the self-consistent LSDA effective potential constrained to have circular symmetry. It is well-known that if the LSDA or HF potentials are not constrained to have the same symmetry as the external potential, situations do arise where they can have a lower symmetry than the external potential. Such calculations are referred to as space unrestricted, and we will use the acronyms ULSDA and UHF for the density functional and Hartree-Fock cases respectively. The ULSDA calculations [7] predict a spin-density wave state, but as pointed out by Hirose and Wingreen this is an artifact of the ULSDA approximation. It is well-known that LSDA wavefunctions need not be eigenstates of $\hat{S}^2$ and ULSDA wavefunctions need not be eigenstates of either $\hat{S}^2$ or $\hat{L}$. For example, a spin-density wave state can be obtained in ULSDA calculations by occupying the orbitals $|n, l, s\rangle = (|0, 3, \frac{1}{2}\rangle + |0, -3, \frac{1}{2}\rangle), (|0, 3, -\frac{1}{2}\rangle - |0, -3, -\frac{1}{2}\rangle), (|1, 1, \frac{1}{2}\rangle + |1, -1, \frac{1}{2}\rangle), (|1, 1, -\frac{1}{2}\rangle - |1, -1, -\frac{1}{2}\rangle)$. (In this expression, the l symmetry is approximate since the single-particle orbitals are not eigenstates of $\hat{l}$ for an effective potential that is not circularly symmetric.) Such a spin density wave is purely an artifact of the ULSDA approach. Of course the true spin-resolved pair correlation function and the pair correlation function exhibit oscillations as observed in exact diagonalization and stochastic variational method

studies [10,15], and these oscillations get stronger at large r_s, but these have only a rough qualitative resemblance to the oscillations in the one-body spin density observed in the ULSDA calculations. For one thing the oscillations in the two-body spin density are present at all r_s whereas in the ULSDA calculations there is a critical r_s below which the oscillations in the one-body spin density vanish [7].

In order to check the sensitivity of our DMC energies to the trial wavefunctions employed, we calculated the ground state energy of the $N = 24$ dot with three different sets of orbitals, those obtained from LDA, LSDA and ULSDA calculations. The three calculations yielded energies that agreed with each other within the statistical error. Also, we see little difference in the DMC energies obtained with single-determinant and multiple-determinant wave functions. Hence it appears likely that the fixed-node errors in our calculations are smaller than the statistical error bars.

We now compare the DMC energies to those obtained from HF and LSDA using the Tanatar-Ceperley parametrization [29] for the correlation energy of the 2-dimensional homogeneous electron gas. For each of the two dots, the error in the HF energies is about 20 times larger than the error of the LSDA energies. This is because the HF approximation totally omits the correlation energy while the LSDA approximates both exchange and correlation, but in these quantum dots the correlation energy is not much smaller than the exchange energy [9]. Also, we note that the percent error we obtain in our HF calculations for the $|L=0, S=2\rangle$ state of the $N = 16$ and the $N = 24$ dots (3.0% and 2.7% respectively), are of the same order of magnitude as the percent error obtained in UHF calculations in reference [6]. The same analysis made on the results included in our previous paper [9] show that the difference between HF and DMC results decreases with the number of electrons N from 11.7% for $N = 2$ electrons to 3.3% for $N = 13$ electrons. Hence, although UHF must yield lower energies than HF, the improvement is not large and the remaining errors are large not only on the scale of the excitation energies but also on the scale of the LSDA errors.

3.2 Charge and spin densities

In Figure 1 we compare the DMC and LSDA spin densities for the ground state of the $N = 16$ dot. The agreement is fairly good and the errors in the spin densities of the two channels tend to cancel so that the total densities, shown in Figure 2 agree better than the spin densities. This happens in the $N = 24$ dot too. In Figure 2 we also show the HF ground state density. It differs greatly from the DMC density, in part because the HF state has $|L=0, S=0\rangle$ symmetry, whereas the DMC state has $|L=0, S=2\rangle$ symmetry, but also because in general it appears that HF tends to yield densities that oscillate more than the true density [9,30].

In Figure 3 we compare densities obtained from DMC, LSDA and HF for the $N = 24$ dot. The $|L=0, S=2\rangle$ DMC

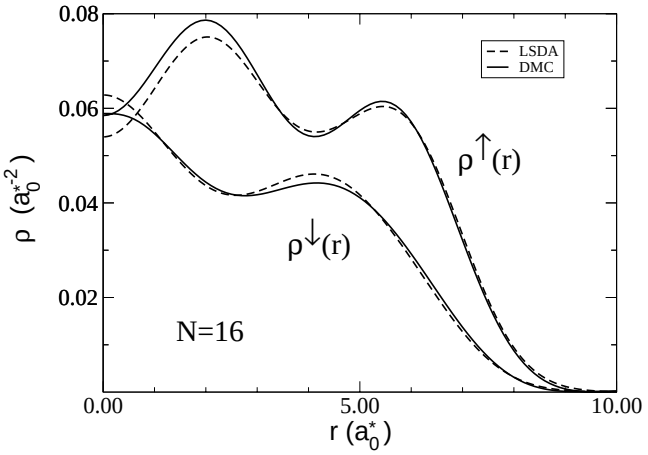

Fig. 1. Comparison of the DMC and LSDA spin densities for the ground state of the $N = 16$ dot. Solid line: DMC; dashed line: LSDA.

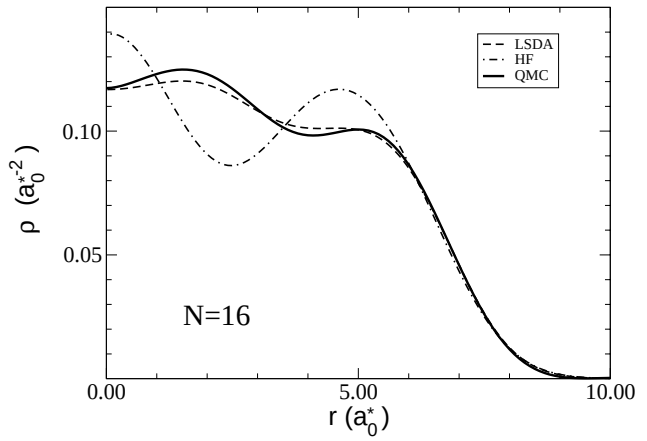

Fig. 2. Comparison of the DMC, LSDA and HF densities for the ground state of the $N = 16$ dot. Solid line: DMC; dashed line: LSDA; dot-dashed line: HF.

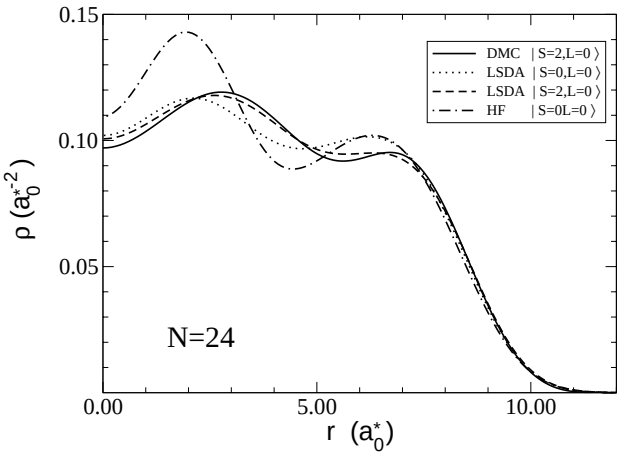

Fig. 3. Comparison of the DMC, LSDA and HF densities for the $N = 24$ dot. Solid line: DMC $|L = 0, S = 2\rangle$; dashed line: LSDA $|L = 0, S = 2\rangle$; dotted line: LSDA $|L = 0, S = 0\rangle$; dot-dashed line: HF $|L=0, S=0\rangle$.

Table 2. DMC Energies (in effective Hartree units) of the low-lying excited states of the $N = 16$ and 24 dots and their difference with the respective ground states energy. The numbers in parenthesis are the statistical errors in the last digit. The finite time-step error for the energies of the $N = 24$ dot may be as large as $0.003H^*$. The $L=0, S=0$ state, shown in boldface, is the ULSDA ground state according to reference [7].

N	L,S	$N_{\rm conf}$	$N_{\rm det}$	DMC Energy	$\Delta E_{\rm excited-ground}$
16	0,1	3	4	41.066(1)	0.020
	4,1	2	4	41.080(1)	0.034
	2,0	3	6	41.081(1)	0.035
	0,0	4	8	41.088(1)	0.042
	2,1	3	6	41.091(1)	0.045
	6,1	1	1	41.093(1)	0.047
	6,0	1	2	41.094(1)	0.048
	4,0	3	5	41.101(1)	0.055
	8,0	1	1	41.113(1)	0.067
24	2,2	1	1	75.995(1)	0.020
	4,2	1	1	76.020(1)	0.045
	0,1	6	7	76.021(1)	0.046
	10,1	1	1	76.022(1)	0.047
	6,0	4	8	76.023(1)	0.048
	2,1	7	8	76.023(1)	0.048
	12,0	1	1	76.026(1)	0.051
	6,1	4	4	76.026(1)	0.051
	4,0	6	12	76.036(1)	0.061
	8,1	2	2	76.039(1)	0.064
	8,0	3	5	76.044(1)	0.069
	0,0	8	16	76.047(1)	0.072
	2,0	6	14	76.052(1)	0.076
	4,1	5	6	76.053(1)	0.077

ground state density agrees well with the $|L=0, S=2\rangle$ excited state LSDA density. It agrees less well with the LSDA $|L=0, S=0\rangle$ ground state since the symmetries are different. The HF ground state also has the wrong symmetry and again its density has oscillations that are too large.

3.3 Excited-state energies

In Table 2 we list the energies of the first several low-lying excited states of the $N = 16$ and $N = 24$ dots. In the case of quantum rings, it has been shown, from exact diagonalization calculations, that the excitation spectrum is close to that resulting from an effective Hamiltonian with rotational, vibrational and spin-spin interaction terms [13]. If

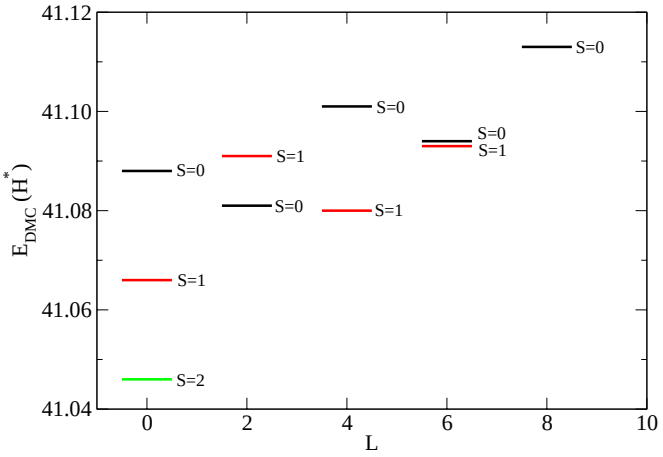

Fig. 4. Energy spectrum for the $N = 16$ dot as function of the total orbital angular momentum.

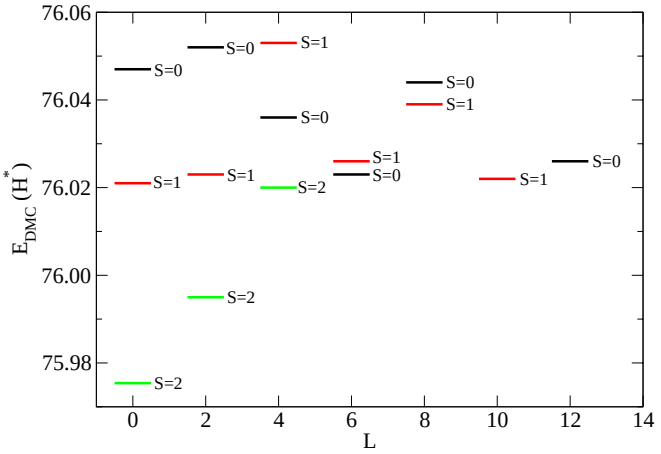

Fig. 5. Energy spectrum for the $N = 24$ dot as function of the total orbital angular momentum.

the energy levels are plotted as a function of the angular momentum, L, the lowest energy states of each L (forming the so-called yrast line) show a roughly parabolic dependence [13] on L, as one would expect for a rigid rotor. In Figures 4 and 5 we plot our calculated energies in a similar fashion, with the spin value shown next to each state. It is apparent that the lowest energy states of each L do not lie on a parabola. This is not surprising – in the case of the quantum rings the moment of inertia is constrained by the radius of the rings (if they are sufficiently narrow) and so is roughly independent of the energy level, whereas in the case of the quantum dots, treated here, the electrons are free to distribute themselves differently for each energy level. In fact, Manninen *et al.* [14] have found that the maximum absolute value of the wave function for a $N = 6$ dot occurs for electron geometries that depend on the angular momentum of the state.

Approximate theories, such as Hartree-Fock or the local spin density approximation, both in the space-restricted and space-unrestricted versions, do not correctly predict the excitation spectra of dots. Although, as seen from Table 1, the LSDA energies are considerably more

accurate than the HF energies, they are certainly not accurate enough for this purpose. For example for the $N = 16$ dot, the ULSDA calculations of Koskinen *et al.* [7] predict a first excitation energy of 9.05 mH* corresponding to a transition from the $|S = 2\rangle$ ground state to the $|S = 0\rangle$ SDW excited state but in our calculations the lowest excitation energy is 20.4 mH* corresponding to a transition from the $|L = 0, S = 2\rangle$ ground state to the $|L = 0, S = 1\rangle$ excited state. For the $N = 24$ dot Koskinen *et al.* [7] find a first excitation energy of 0.36 mH* from the $|S = 0\rangle$ SDW ground state to the $|S = 2\rangle$ excited state whereas we find an excitation energy of 16.5 mH* corresponding to a transition from the $|L=0, S=2\rangle$ ground state to the $|L=2, S=2\rangle$ excited state.

4 Conclusions

We have used diffusion Monte Carlo to calculate ground and excited state energies, and spin densities of two dots ($N = 16, 24$) for which approximate calculations (UHF and ULSDA) were available but exact diagonalization studies are not feasible. We find that LSDA energies and spin densities are more accurate than those from HF, but that even LSDA does a poor job of predicting excitation energies and can even predict the wrong symmetry for the ground state. The LSDA spin densities are in good agreement with DMC spin densities in the case of $N = 16$ where the two methods predict the same spin polarization. Unlike the case of quantum rings, the energy levels of the dots are not well described by an effective Hamiltonian containing rotational, vibrational and spin-spin interaction terms.

Calculations were partly performed on a Cray T3E computer at Cineca-Bologna, Italy under an INFM grant for Parallel Computing Initiative. We thank T. Puente and Ll. Serra for providing us the HF code and the orbitals from the ULSDA calculation. This work is funded in part by Sandia National Laboratory. Sandia is a multiprogram laboratory operated by Sandia Corporation, a Lockheed Martin Company, for the United States Department of Energy, under Contract No. DEAC0494AL85000.

Appendix A: Construction of S^2 eigenfunctions

We wish to construct simultaneous eigenstates of $\hat{L} \equiv \hat{L}_z$, $\hat{S}_z$ and $\hat{S}^2$. Single determinants are eigenstates of $\hat{L}_z$ and $\hat{S}_z$ but not necessarily of $\hat{S}^2$. Consequently, we need to diagonalize the matrix representation of $\hat{S}^2$ in the basis of determinants having the desired L_z and S_z quantum numbers. The following identity facilitates the calculation of the matrix representation of $\hat{S}^2$.

A.1: The Dirac identity

For a many-electron system the total spin operator is the sum of one-electron operators:

$$\hat{S} = \sum_{i=1}^{N} \hat{S}(i), \tag{12}$$

and the square of the total spin operator is given by the relation

$$\hat{S}^2 = \hat{S}_x^2 + \hat{S}_y^2 + \hat{S}_z^2 = \hat{S}_+\hat{S}_- + \hat{S}_z^2 - \hat{S}_z = \hat{S}_-\hat{S}_+ + \hat{S}_z^2 + \hat{S}_z. \tag{13}$$

Using (12) and (13), we can write

$$\begin{aligned}\hat{S}^2 &= \sum_{i=1}^{N} \hat{S}^2(i) + 2\sum_{i<j}^{N} \Big[\hat{S}_x(i)\hat{S}_x(j) \\ &\quad + \hat{S}_y(i)\hat{S}_y(j) + \hat{S}_z(i)\hat{S}_z(j)\Big] \\ &= \sum_{i=1}^{N} \hat{S}^2(i) + 2\sum_{i<j}^{N} \hat{S}(i)\cdot\hat{S}(j) \\ &= \sum_{i=1}^{N} \hat{S}^2(i) + \sum_{i<j}^{N} \Big[\hat{S}_+(i)\hat{S}_-(j) \\ &\quad + \hat{S}_-(i)\hat{S}_+(j) + 2\hat{S}_z(i)\hat{S}_z(j)\Big]. \end{aligned} \tag{14}$$

Operating on the four primitive two-electron spin functions with $\hat{S}(1)\cdot\hat{S}(2)$ yields:

$$\begin{aligned}\Big[\hat{S}(1)\cdot\hat{S}(2)\Big]\ \chi^{\uparrow}(1)\chi^{\uparrow}(2) &= \tfrac{1}{4}\chi^{\uparrow}(1)\chi^{\uparrow}(2) \\ &= \left(\tfrac{\hat{P}_{12}^{\sigma}}{2} - \tfrac{\hat{I}}{4}\right)\chi^{\uparrow}(1)\chi^{\uparrow}(2) \\ \Big[\hat{S}(1)\cdot\hat{S}(2)\Big]\ \chi^{\uparrow}(1)\chi^{\downarrow}(2) &= \tfrac{1}{2}\chi^{\downarrow}(1)\chi^{\uparrow}(2) - \tfrac{1}{4}\chi^{\uparrow}(1)\chi^{\downarrow}(2) \\ &= \left(\tfrac{\hat{P}_{12}^{\sigma}}{2} - \tfrac{\hat{I}}{4}\right)\chi^{\uparrow}(1)\chi^{\downarrow}(2) \\ \Big[\hat{S}(1)\cdot\hat{S}(2)\Big]\ \chi^{\downarrow}(1)\chi^{\uparrow}(2) &= \tfrac{1}{2}\chi^{\uparrow}(1)\chi^{\downarrow}(2) - \tfrac{1}{4}\chi^{\downarrow}(1)\chi^{\uparrow}(2) \\ &= \left(\tfrac{\hat{P}_{12}^{\sigma}}{2} - \tfrac{\hat{I}}{4}\right)\chi^{\downarrow}(1)\chi^{\uparrow}(2) \\ \Big[\hat{S}(1)\cdot\hat{S}(2)\Big]\ \chi^{\downarrow}(1)\chi^{\downarrow}(2) &= \tfrac{1}{4}\chi^{\downarrow}(1)\chi^{\downarrow}(2) \\ &= \left(\tfrac{\hat{P}_{12}^{\sigma}}{2} - \tfrac{\hat{I}}{4}\right)\chi^{\downarrow}(1)\chi^{\downarrow}(2) \end{aligned} \tag{15}$$

where $\hat{P}_{12}^{\sigma}$ is the spin permutation operator. So, we obtain the Dirac identity

$$\hat{S}(1)\cdot\hat{S}(2)\chi(1,2) = \left(\frac{\hat{P}_{12}^{\sigma}}{2} - \frac{\hat{I}}{4}\right)\chi(1,2), \tag{16}$$

or,

$$\hat{S}^2\chi(1,2) = \left(\hat{I} + \hat{P}^{\sigma}_{12}\right)\chi(1,2), \tag{17}$$

where $\chi(1,2)$ is an arbitrary two-electron spin functions. In the many-electron case we obtain from equations (14) and (16):

$$\begin{aligned}
&\hat{S}^2\chi(1,\ldots,N) = \\
&\quad\left[\sum_{i=1}^{N}\hat{S}^2(i) + 2\sum_{i<j}^{N}\hat{S}(i)\cdot\hat{S}(j)\right]\chi(1,\ldots,N) \\
&= \left[N\frac{3}{4}\hat{I} + 2\left(\sum_{i<j}^{N}\frac{\hat{P}^{\sigma}_{ij}}{2} - \frac{N(N-1)}{2}\frac{\hat{I}}{4}\right)\right]\chi(1,\ldots,N) \\
&= \left[\frac{-N(N-4)}{4}\hat{I} + \sum_{i<j}^{N}\hat{P}^{\sigma}_{ij}\right]\chi(1,\ldots,N),
\end{aligned} \tag{18}$$

where $\chi(1,\ldots,N)$ is an arbitrary spin function in the 2^N-dimensional spin space of N electrons. The matrix elements of $\hat{S}^2$ can be calculated from either equation 14 or equation 18, the latter being somewhat simpler.

A.2: An example

As an example, we construct the $L=4, S=1$ configuration state functions of the 24-electron dot. There are $N = 4$ open-shell electrons and (18) reduces to

$$\hat{S}^2\chi = \sum_{i<j}\hat{P}^{\sigma}_{ij}\chi. \tag{19}$$

There are six determinants with $L=4$ and $S_z = 1$:

$$\begin{aligned}
D^{\uparrow}_1\, D^{\downarrow}_1 &= |4^{\uparrow}, 2^{\uparrow}, -2^{\uparrow}|\,|0^{\downarrow}| \\
D^{\uparrow}_2\, D^{\downarrow}_2 &= |4^{\uparrow}, 2^{\uparrow}, 0^{\uparrow}|\,|2^{\downarrow}| \\
D^{\uparrow}_3\, D^{\downarrow}_3 &= |4^{\uparrow}, -2^{\uparrow}, 0^{\uparrow}|\,|2^{\downarrow}| \\
D^{\uparrow}_4\, D^{\downarrow}_4 &= |2^{\uparrow}, -2^{\uparrow}, 0^{\uparrow}|\,|4^{\downarrow}| \\
D^{\uparrow}_5\, D^{\downarrow}_5 &= |4^{\uparrow}, -4^{\uparrow}, 2^{\uparrow}|\,|2^{\downarrow}| \\
D^{\uparrow}_6\, D^{\downarrow}_6 &= |4^{\uparrow}, -4^{\uparrow}, 0^{\uparrow}|\,|4^{\downarrow}|.
\end{aligned} \tag{20}$$

The matrix representation of the operator $\hat{S}^2$ is

$$\hat{S}^2 = \begin{pmatrix}
3&1&1&1&0&0\\
1&3&1&1&0&0\\
1&1&3&1&0&0\\
1&1&1&3&0&0\\
0&0&0&0&2&0\\
0&0&0&0&0&2
\end{pmatrix} \tag{21}$$

and its eigenvalues and eigenvectors are

$$\begin{array}{cc}
\text{Eigenvalue } S(S+1) & \text{Eigenvectors} \\
 & \chi_1,\chi_2,\chi_3,\chi_4,\chi_5,\chi_6 \\
2 & \left\{\begin{array}{l}(-1,1,0,0,0,0)\\(-1,0,1,0,0,0)\\(-1,0,0,1,0,0)\\(0,0,0,0,1,0)\\(0,0,0,0,0,1)\end{array}\right. \\
(i.e.\ S=1) & \\
6 & \{\,(1,1,1,1,0,0). \\
(i.e.\ S=2) &
\end{array} \tag{22}$$

Consequently,

$$\Xi^{S=1}_{L=4} = \beta_1\chi_1 + \beta_2\chi_2 + \beta_3\chi_3 + \beta_4\chi_4 + \beta_5\chi_5 + \beta_6\chi_6 \tag{23}$$

where $\beta_1 = -\beta_3 - \beta_4 - \beta_5$. Note that as a by-product we have obtained also the eigenfunction of the $L=4, S=2, S_z=1$ state. However, this is a 4-determinant function and since the energies are independent of S_z it is preferable to use the 1-determinant eigenfunction of the $L=4, S=2, S_z=2$ state.

References

1. U. Meirav, M.A. Kastner, S.J. Wind, Phys. Rev. Lett. **65**, 771 (1990)
2. R.C. Ashoori *et al.*, Phys. Rev. Lett. **68**, 3088 (1992)
3. S. Tarucha *et al.*, Phys. Rev. Lett. **77**, 3613 (1996)
4. D.G. Austing *et al.*, Phys. Rev. **60**, 11514 (1999)
5. C. Yannouleas, U. Landman, Phys. Rev. Lett. **82**, 5325 (1999)
6. B. Reusch, W. Häusler, H. Grabert, Phys. Rev. B. **63**, 113313 (2001)
7. M. Koskinen, M. Manninen, S.M. Reimann, Phys. Rev. Lett. **79**, 1389 (1997)
8. K. Hirose, N.S. Wingreen, Phys. Rev. B **59**, 4604 (1999)
9. F. Pederiva, C.J. Umrigar, E. Lipparini, Phys. Rev. B **62**, 8120 (2000)
10. S.M. Reimann, M. Koskinen, M. Manninen, Phys. Rev. B. **62**, 8108 (2000)
11. P.A. Maksym, T. Chakraborty, Phys. Rev. Lett. **65**, 108 (1990); D. Pfannkuche, V. Gudmundsson, P.A. Maksym, Phys. Rev. B **47**, 2244 (1993); P. Hawrylak, D. Pfannkuche, Phys. Rev. Lett. **70**, 485 (1993); J.J. Palacios, L. Martin-Moreno, G. Chiappe, E. Louis, C. Tejedor, Phys. Rev. B **50**, 5760 (1994); M. Eto, Jpn J. Appl. Phys. **36**, 3924 (1997)
12. A. Wojs, P. Hawrylak, Phys. Rev. B **53**, 10841 (1996)
13. M. Koskinen, M. Manninen, B. Mottelson, S.M. Reimann, Phys. Rev. B **63**, 205323 (2001)
14. M. Manninen, S. Viefers, M. Koskinen, S.M. Reimann, Phys. Rev. B. **64**, 245322 (2001)

15. K. Varga, P. Navratil, J. Usukura, Y. Suzuki, Phys. Rev. B **63**, 205308 (2001).
16. R. Egger, W. Häusler, C.H. Mak, H. Grabert, Phys. Rev. Lett. **82**, 3320 (1999)
17. J. Harting, O. Mülken, P. Borrmann, Phys. Rev. B **62**, 3320 (2000)
18. The $|L=0, S=0\rangle$ state of the $N=4$ dot was the only one that did not agree, for reasons that we do not understand Since the DMC energy was the lower one for this state, the discrepancy cannot be due to the fixed-node error
19. V. Fock, Z. Phys. **47**, 446 (1928); C.G. Darwin, Proc. Cambridge Philos. Soc. **27**, 86 (1930)
20. A. Puente, Ll. Serra, Phys. Rev. Lett. **83**, 3266 (1999)
21. C.J. Umrigar, M.P. Nightingale, K.J. Runge, J. Chem. Phys. **99**, 2865 (1993)
22. J.B. Anderson, J. Chem. Phys. **63**, 1499 (1975); *ibid.* **65**, 4121 (1976)
23. G. Ortiz, D.M. Ceperley, R.M. Martin, Phys. Rev. Lett. **71**, 2777 (1993)
24. F. Bolton, Phys. Rev. **54**, 4780 (1996)
25. See W.M.C. Foulkes, R.Q. Hood, R.J. Needs, Phys. Rev. B **60**, 4558 (1999) for an example where the energy obtained need not be an upper bound
26. P. Ballone, C.J. Umrigar, P. Delaly, Phys. Rev. B **45**, 6293 (1992)
27. C-J. Huang, C. Filippi, C.J. Umrigar, J. Chem. Phys. **108**, 8838 (1998)
28. C.J. Umrigar, K.G. Wilson, J.W. Wilkins, in *Computer Simulation Studies in Condensed Matter Physics: Recent Developments*, edited by D.P. Landau, H.B. Schüttler (Springer-Verlag, Berlin, 1988); C.J. Umrigar, K.G. Wilson, J.W. Wilkins, Phys. Rev. Lett. **60**, 1719 (1988)
29. B. Tanatar, D.M. Ceperley, Phys. Rev. B **39**, 5005 (1989)
30. The HF approximation gives oscillations that are a bit too large for atomic densities as well. See, *e.g.*, C. Filippi, X. Gonze, C.J. Umrigar, *Recent Developments and Applications of Density Functional Theory*, edited by J.M. Seminario (Elsevier, Amsterdam, 1996)